

An α -1,3-Mannosyltransferase of *Cryptococcus neoformans**

Received for publication, July 7, 2003, and in revised form, September 11, 2003
Published, JBC Papers in Press, September 21, 2003, DOI 10.1074/jbc.M307223200

Ulf Sommer[‡], Hong Liu, and Tamara L. Doering[§]

From the Department of Molecular Microbiology, Washington University Medical School, St. Louis, Missouri 63110

***Cryptococcus neoformans* is a pathogenic fungus, distinguished by an elaborate polysaccharide capsule that is essential for its virulence. As part of an effort to understand the biosynthesis of this important structure, we initiated purification of an α -1,3-mannosyltransferase with appropriate specificity for a role in building the main capsule polysaccharide, glucuronoxylomannan. A pool of proteins that was 5,000-fold enriched in this activity included several polypeptides, which acted potentially as the catalytic protein. These were analyzed using sequence information and double-stranded RNA interference. Interference that targeted a sequence corresponding to part of a 46 kDa protein in the enriched fraction abolished the activity of interest and reduced the capsule on the affected cells. This gene was cloned and expressed in active form in *Saccharomyces cerevisiae* to confirm function, and was termed *CMT1*, for cryptococcal mannosyltransferase 1. *CMT1* has no confirmed homologs in GenBankTM other than *CAP59*, a cryptococcal gene encoding a protein of unknown function that is required for capsule synthesis and virulence. The *Cmt1p* protein also co-purifies with a homolog of *CAP64*, a gene whose product has similarly been implicated in capsule synthesis and virulence. A strain disrupted in *CMT1* was generated in *C. neoformans*; this had no effect on virulence in an animal model of cryptococcosis.**

Cryptococcus neoformans is a fungal pathogen responsible for serious disease and lethal meningitis, primarily in the setting of compromised immunity (1). Its major virulence factor is an extensive polysaccharide capsule (2) that has been implicated in evasion of host immune defenses (3, 4). The capsule has two major components, termed glucuronoxylomannan (GXM,¹ ~90% of the capsule mass) and galactoxylomannan (GalXM, ~7% of the capsule mass). The former, with an estimated molecular mass of over a million daltons, consists of a linear mannan in α -1,3-linkage. The mannose residues are decorated with glucuronic acid (linked β -1,2) and xylose (linked β -1,2 and β -1,4) in a mannose/glucuronic acid/xylose ratio of

3:1:1–4. The amount of xylose present, as well as the extent of 6-O-acetylation of the mannose backbone, varies with the serotype of the organism (5). The galactoxylomannan, with an estimated mass of ~100,000 daltons, is a more complex structure, with an α -1,3-galactose backbone bearing side chains consisting of 3–6 residues of mannose and xylose (6). The capsule is regulated, with its size dependent on growth conditions *in vitro* and tissue site *in vivo*.

Because of the critical importance of the capsule to the pathogenesis of cryptococcosis, there has been substantial effort to understand how it is synthesized and assembled on the cell surface. One approach has been to screen mutagenized cells for those that either do not express capsule at all (7, 8) or produce altered capsule as indicated by reduced binding of monoclonal antibodies (9–12). Molecular studies of these mutants have identified an array of genes whose products are clearly required for normal capsule synthesis (9, 10, 13–16), but whose specific functions are not known. Biochemical approaches have conversely detected enzyme activities that must be involved in building capsule, but the corresponding protein sequences are not known (17–19). In only a few cases have molecular and biochemical techniques been used together to identify enzymes required for capsule synthesis and characterize their role in virulence (10, 20, 21).

Many of the enzymes involved in capsule synthesis are sugar transferases that generate the unique structures of GXM and GalXM (17, 18, 22). We are specifically interested in the mannosyltransferase, which generates the α -1,3-linked backbone of the more abundant capsule polymer, GXM. This activity is presumably required at the start of GXM synthesis; without it this critical polymer should not be made. Although the genome sequence of *C. neoformans* has recently been obtained (23), it is difficult to identify such an enzyme by homology to genes in other organisms (24). For example, sequence analysis may suggest a mannosyltransferase, but it would be impossible to predict what linkage the putative protein might generate and what substrate it would prefer. Further, fungi typically encode numerous mannosyltransferases, as they generate abundant mannose linkages during formation of GPI anchors, glycoproteins, and glycolipids (25–29).

To identify the α -1,3-mannosyltransferase, which generates the GXM backbone, we began with a biochemical approach. In previous studies we identified both α -1,2 and α -1,3 mannosyltransferase activities in crude preparations of cryptococcal membranes, monitoring activity by transfer of radioactive mannose from a tritiated GDP-mannose donor to a mannose- α -1,3-mannose acceptor (22). Our goal in the current work was to purify the α -1,3 mannosyltransferase in sufficient quantities to obtain sequence information, and to examine the effect of altering this activity on capsule formation and cryptococcal virulence. This should enable a better understanding of the fascinating biochemistry involved in capsule synthesis, and inform efforts to identify anti-fungal compounds.

* This work was supported by National Institutes of Health Grant R01 AI49173 and a GRANT Award from Neose Technologies, and the Andrew and Virginia Craig Faculty Research Fund. The costs of publication of this article were defrayed in part by the payment of page charges. This article must therefore be hereby marked "advertisement" in accordance with 18 U.S.C. Section 1734 solely to indicate this fact.

[‡] Current address: Mass Spectrometry Resource, Boston University School of Medicine, Boston, MA.

[§] A Burroughs Wellcome Fund Junior Investigator in Molecular Pathogenic Mycology. To whom correspondence should be addressed: Campus Box 8230, 660 South Euclid Ave., St. Louis, MO 63110-1093. Tel.: 314-747-5597; Fax: 314-362-1232; E-mail: doering@borcim.wustl.edu.

¹ The abbreviations used are: GXM, glucuronoxylomannan; PBS, phosphate-buffered saline; HPLC, high performance liquid chromatography; conA, concanavalin A; CMT1, cryptococcal mannosyltransferase 1.

EXPERIMENTAL PROCEDURES

Materials—Generous gifts of non-commercial reagents included GXM-derived mannan from R. Cherniak, GDP-hexanolamine resin from G. Hart (Johns Hopkins University School of Medicine) and monoclonal anti-capsule antibodies 2H1 (30) and 3C2 (31) from A. Casadevall (Albert Einstein School of Medicine) and T. Kozel (University of Nevada at Reno), respectively. α -1,3-D-Mannobiose was from V-Labs, Inc. (Covington, LA), medium components were from BD Pharmingen or Bio101 (Carlsbad, CA), and other materials, including anti-His antibody, were from Sigma Chemical Co. Polyclonal rabbit antiserum against bacterially expressed Cmt1p (see below) was generated at Covance Laboratories, (Denver, PA).

Strains and Cell Growth—Wild type *C. neoformans* strains H99 (serotype A) and the acapsular mutant strain Cap67 (8) were from A. Casadevall (Albert Einstein College of Medicine); *C. neoformans* JEC43 (serotype D *MAT α ura*) was provided by J. Heitman (Duke University Medical College); *Saccharomyces cerevisiae* strain TDY172 (RSY620; *MAT α ade2-1 trp1-1 leu2-3,112 ura3-1 his3-11,15 pep4::TRP1*) was from R. Schekman (University of California at Berkeley); and *Tremella mesenterica* Fries was from the American Type Culture Collection. Cell growth was as indicated in YPD (1% Bacto Yeast Extract, 2% Bacto Peptone, 2% dextrose), YM (0.3% Bacto Yeast Extract, 0.3% Bacto Malt Extract, 0.5% Bacto Peptone, 1.3% dextrose), minimal medium lacking uracil or minimal medium containing 1 g/liter of 5-fluoro-orotic acid (32). For small scale cultures growth was at 30 °C (or room temperature for *T. mesenterica*) with continuous shaking (200 rpm), and was monitored by turbidity at 600 nm. For large scale preparations a 50-ml overnight culture of *C. neoformans* strain Cap67 in YPD was used to inoculate a 1.5 liters of overnight culture in YPD. This was then used to inoculate a 30-liter fermenter containing YPD medium, in which cells were grown at 30 °C to an OD₆₀₀ of ~40. Cells (~2 kg wet weight) were harvested by centrifugation (15 min, 4 °C, 2000 \times g), washed once in cold distilled water, and resuspended in 0.3 volumes cold distilled water. The cell suspension was frozen by pouring a thin stream into liquid nitrogen with constant stirring, and stored at -70 °C until use.

Mannosyltransferase Assays—Activity was assayed by monitoring the conversion of anthranilic acid derivatized α -1,3-mannobiose to the corresponding mannotriose. The derivatized mannoside was prepared as in Ref. 33, and purified on a RP-18 column (HAISIL HL C18, 5 μ m, 4.6 \times 250 mm) by sequential runs in (a) 10% acetonitrile/90% 0.25% 1-butylamine, 0.5% phosphoric acid, 1% tetrahydrofuran in water and (b) 8% acetonitrile/92% water, with fluorescence detection at $\lambda_{\text{ex}} = 360$ nm and $\lambda_{\text{em}} = 425$ nm. The standard assay mixture (25 μ l) included 5 μ l of protein sample, ~1 mM derivatized mannoside, 0.2 mg/ml GDP-mannose, 10 mM CoCl₂ (or other cation as indicated), and 50 mM Tris, pH 8. The reaction was incubated for 1 h at 30 °C, terminated by the addition of 4 volumes of 0.1% acetic acid in acetonitrile, and subjected to centrifugation to remove any particulate material. 100 μ l of the supernatant fraction was analyzed on a TosoHaas TSK-Gel Amide 80 column (4.6 \times 250 mm, 5 μ m) using solvents A (0.2% triethylamine, 0.2% acetic acid in water) and B (0.1% acetic acid in acetonitrile) in Program 1 (10 min 20% A, 80% B followed by a 15-min linear gradient to 70% A, 30% B and holding at that composition), Program 2 (5 min 20% A, 80% B followed by a 20-min linear gradient to 60% A, 40% B and holding at that composition), or Program 3 (isocratic at 19% A, 81% B). Fluorescent product oligosaccharides were detected at $\lambda_{\text{ex}} = 230$ nm, $\lambda_{\text{em}} = 425$ nm. Standards for mannosyl transfer reactions were derived from authentic α -1,3-mannan of *C. neoformans*, a generous gift of R. Cherniak. This material was subjected to repeated partial hydrolysis (1 h; 95 °C; 0.1 M HCl) and then derivatized and purified as above.

Mannosyltransferase Purification—All steps were carried out on ice or at 4 °C, unless indicated otherwise.

Buffers—All buffers were prepared at room temperature, then filtered and chilled before use. Buffer A, 50 mM Tris, pH 8.0, 50 mM NaCl, 0.1 mM EDTA, 1% Triton X-100. Buffer B, 50 mM Tris, pH 8, 100 mM NaCl, 0.1 mM EDTA, 0.2% Triton X-100. Buffer C was prepared as buffer B but with 400 mM NaCl. Buffer D, 50 mM Hepes, pH 8, 0.2% Triton X-100. Buffer E, as buffer D but with 500 mM NaCl. Buffer F, 50 mM Tris, pH 8, 100 mM NaCl, 0.1 mM Triton X-100. Buffer G, 50 mM Tris, pH 8, 500 mM NaCl, 0.1 mM Triton X-100. Buffer H1, 50 mM Tris, pH 8, 12.5 mM K-PO₄, pH 6.8, 0.1% Triton X-100. Buffer H5, as Buffer H1 but with 200 mM K-PO₄. Buffer I, 20 mM Tris, pH 7.5, 500 mM NaCl, 0.1% Triton X-100, 1 mM CaCl₂, and 1 mM MnCl₂. Buffer J, 20 mM Tris, pH 7.5, 100 mM NaCl, 200 mM α -methyl-mannoside, 0.1% Triton X-100. Buffer K, 20 mM Tris, pH 7.5, 100 mM NaCl, 500 mM α -methyl-mannoside, 0.1% Triton X-100.

Membrane Preparation—300 g of frozen cells (Cap67, see Ref. 22 for

details of strain choice) were lysed by processing with liquid nitrogen in a Waring blender. The resulting powder was suspended in a final volume of 900 ml in 50 mM Tris, pH 8, 0.5 mM phenylmethylsulfonyl fluoride, 1 mM EDTA. After a clearing spin to remove cell debris, the supernatant fraction was subjected to centrifugation (100,000 \times g, 1 h). The resulting pellet was resuspended in ~350 ml of the same buffer, and again subjected to centrifugation (125,000 \times g, 1 h). This pellet, along with loose material that sedimented just above it, was resuspended in 20 ml of the same buffer and either frozen at -70 °C for future use or rotated end-over-end overnight for complete resuspension before detergent solubilization. For smaller scale membrane preparation, lysis was with glass beads, either in a Bead Beater (Biospec Products, Bartlesville, OK) or by vortex mixing as in Ref. 22.

Solubilization—20% Triton X-100, 50 mM Tris, pH 8 was added to the large-scale membrane preparation to yield a final detergent concentration of 2%. The resulting suspension was rotated end-over-end for 1 h, subjected to centrifugation (125,000 \times g, 15 min), and the supernatant fraction (SolZ) recovered.

Q Sepharose Chromatography—The SolZ fraction was applied to a Q Sepharose Fast Flow column (10 \times 300 mm, flow rate 0.8 ml/min), and the column washed with buffers A and B. Activity was eluted with a 120-ml linear gradient from buffer B to buffer C.

Source 15Q Chromatography—The most active fractions from Q Sepharose chromatography were pooled, diluted with an equal volume of distilled water, and applied at 2 ml/min to a 16 \times 200 mm HPLC column that had been packed with Source 15Q resin (Amersham Biosciences), equilibrated with buffer D, and kept on ice. The column was washed with 90% buffer D, 10% buffer E, and the activity was eluted with an 80 ml linear gradient from the same mixture to 50% buffer D, 50% buffer E.

Hydroxyapatite Chromatography—The most active fractions from Source15Q chromatography were pooled, and directly applied to a 2.5 ml ($d = 7$ mm) Hydroxyapatite Ultrogel column. The column was washed with buffers F, G, and H1 and activity was eluted with a 20-ml linear gradient from buffer H1 to buffer H5.

Concanavalin A Chromatography—The most active hydroxyapatite fractions were pooled and incubated with 1 ml of concanavalin A-agarose (Amersham Biosciences) that had been prewashed with 2 M α -methyl mannoside and water, and pre-equilibrated with buffer I. After 1 h of rotation the resin was poured into a column and washed (gravity flow) with buffer I followed by 25 mM Tris, pH 7.5, 0.1% Triton X-100. Activity was eluted with 20 ml of buffer K.

Second Source 15Q Chromatography—The eluates of the concanavalin A column were pooled, diluted with an equal volume of distilled water, and applied at 1 ml/min to a 1-ml column packed with Source 15Q resin pre-equilibrated with buffer D and kept on ice. After loading, the column was washed with 50% water, 40% buffer D/10% buffer E, and the activity was eluted with a 10-ml linear gradient from that mixture to 50% water, 50% buffer E. The fraction with highest specific activity was used for protein sequencing and characterization.

Protein Sequencing—Edman degradation was performed by Midwest Scientific (St. Louis, MO), and mass spectrometry was performed by Oxford Glycosciences or by the Keck Facility at Yale University.

RNA Interference Studies, Cloning—Based on the peptide sequences obtained from each band of interest (*single* and *double asterisk* in Fig. 2), and sequence analysis as described in the text, we obtained putative coding sequences for the corresponding proteins. To direct interference we chose regions of the sequence that were not predicted to contain introns, and therefore should correspond to mRNA of the genes. Constructs were based on plasmid pCAP59/ADE2i (34), which was modified to eliminate the *NdeI* site downstream of the promoter and the *BglII* site upstream of the terminator. To target *CMT1*, the first 282 bp of the predicted coding sequence were PCR-amplified from JEC43 cDNA, using primers 5'-GGAATTCCATATGTTCCGAAATACCC-3' and 5'-CGCCTAGGTCTAAACGCTTCTGATGTCG-3' to incorporate *NdeI* and *AvrII* sites at the 5'- and 3'-ends of the product (product A). Product A was digested with those enzymes and ligated into the similarly restricted plasmid pCAP59/ADE2i, replacing the *CAP59* sequences with those from *CMT1* to yield product B, which was then amplified in *Escherichia coli*. Product A was additionally amplified using primers designed to incorporate *BglII* and *XhoI* sites at the 5'- and 3'-ends, respectively, to form product C. Product C was digested with *BglII* and *XhoI* and ligated to similarly restricted product B. The resulting plasmid, pCMT1/ADE2i, contained inverted repeats of *CMT1* separated by a portion of GFP as a spacer, and flanked by inverted repeats of a portion of *ADE2* as well as the actin promoter and *gal7* terminator. To target the *CAP64* homolog a parallel strategy was used to generate pCAP64H/ADE2i, except using primers 5'-GGAATTCCATATGTTTC-

CTGGCCAACGGCAAG-3' and 5'-CCGCCTAGGCGTCCAATGTTGTAAGGC-3' to amplify the first 335 bp of the putative coding region. Details of all cloning manipulations are available from the authors.

Transformation and Analysis—Transformation into JEC43 cells was as described (34). Transformants that turned pink, indicative of functioning RNAi targeting *ADE2*, were chosen for further analysis. Several individual transformants were restreaked on both medium lacking uracil to maintain the interference plasmid and on medium containing uracil and 5-fluoro-orotic acid (5-FOA) to select against plasmid maintenance. These pairs of strains, the latter of which reverted to white colony type, were then used for membrane preparations and activity assays. Control strains included transformants with pCAP59/*ADE2i*, which targets both the *CAP59* and *ADE2* genes, and strains containing p*ADE2i*, which targets *ADE2* alone (34).

Obtaining Gene Sequence for *CMT1*—Based on alignment of peptide sequences (Table II) to predicted protein sequence from *C. neoformans* (see text), gene specific primers were designed to obtain the entire *CMT1* coding sequence by RT-PCR. Briefly, total RNA was isolated from *C. neoformans* serotype D strain Cap67, reverse-transcribed using an oligo(dT) primer, and used as a template for rapid amplification of cDNA ends (RACE) analysis using Clontech Marathon reagents as directed by the manufacturer. Gene specific primers for 5'- and 3'-RACE reactions were as-1 (5'-GTGCGAGTCGCTGGAAGGTCCTCC-3') and s-1 (5'-GGACCTCTTCTGGAAAGGGCGCT-3'), respectively. RACE reaction products were sequenced and assembled into a contiguous region, with initiation and stop codons bounding an ORF. The full length ORF (1401 bp) was then amplified using primers MT48-s3 (5'-GGAATTCATATGTTCCGAAATACCC-3') and MT48-as3 (5'-CTAGCTAGCTCATTCTAACCAGGGC-3') to incorporate restriction sites for further cloning. Additional cloning details are available from the authors, and the coding sequence has been submitted to GenBank™ (accession no. AY380340).

Expression in *S. cerevisiae*—A His-tagged, truncated version of *Cmt1p* was generated by PCR amplification of the coding sequence from nucleotide 220 through to the protein C terminus, incorporating a 6-His coding sequence at the N terminus as well as EcoRI and HindIII restriction sites at the 5'- and 3'-ends, respectively. Primers used for amplification were 5'-CCGGAATTCATGCATCATCATCATCACAGCAGCGGCCTGGTGGCGCGCGGCAGCGTGATACATACCAAGGACCTC-3' and 5'-CCCAAGCTTTCATTCTAACCAGGGCTGTAC-3'. The product was digested with EcoRI and HindIII and cloned into a 2 μ expression vector between the promoter and transcriptional terminator of phosphoglycerate kinase (plasmid pPGK, Ref. 35, from K. Blumer, Washington University Medical School). The resulting plasmid or the starting vector alone were transformed into TDY172 by electroporation using standard methods, and cells containing the *URA3* marked plasmid were selected on medium lacking uracil for further analysis.

Gene Disruption and Deletion—*CMT1* was disrupted following the basic protocol described in (36), using a disruption cassette consisting of nucleotides -305 to 657 of *CMT1*, the cryptococcal serotype D *URA5* gene in reverse orientation, and nucleotides 817 through +346 of *CMT1*. For deletion the cassette consisted of nucleotides -1042 to -1 of *CMT1*, the same marker, and nucleotides +1 to +1018 of *CMT1*. Each cassette was constructed by PCR (primer sequences available from the authors), purified, and biologically transformed (37, 38) into JEC43 cells, which were then plated onto medium lacking uracil and incubated at 30 °C for 3–5 days to allow colony growth. Colonies were screened as described in the text to identify those in which endogenous *CMT1* was successfully replaced.

Electron Microscopy—For ultrastructural analysis, yeast cells were fixed in 2% glutaraldehyde (Polysciences Inc., Warrington, PA) in 100 mM phosphate buffer, pH 7.2 for 2 h at 4 °C. Cells were washed in phosphate buffer and postfixed in 1% osmium tetroxide (Polysciences Inc.) for 1 h at 4 °C. Samples were then rinsed in buffer, followed by dehydration in a graded series of ethanol and propylene oxide prior to embedding in Eponate 12 resin (Ted Pella Inc., Redding, CA). Samples were sectioned with a Leica Ultracut UCT ultramicrotome (Leica Microsystems Inc., Bannockburn, IL). 70–90 nm sections were immunolabeled with mouse monoclonal antibody 2H1 (30) followed by 18 nm colloidal gold-conjugated goat anti-mouse IgG. Sections were stained with uranyl acetate and lead citrate and viewed with on a JEOL 1200EX transmission electron microscope (JEOL USA Inc., Peabody, MA). All labeling experiments were processed in parallel with controls omitting the primary antibody. These controls were consistently negative at the concentration of gold-conjugated secondary antibodies used in these studies.

Mouse Studies—Groups of 8 4–6-week-old female C57Bl/6 mice (National Cancer Institute) were anesthetized and 2 \times 10⁴ PBS-washed

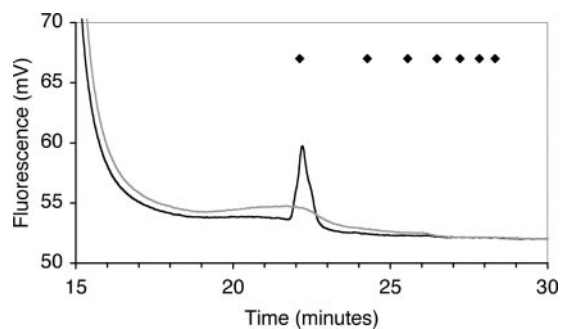


FIG. 1. **Mannosyltransferase assay.** Fluorescent dimannoside substrate was incubated with cryptococcal membranes in the presence (*black trace*) or absence (*gray trace*) of GDP-mannose, and analyzed by Program 1. *Diamonds* indicate the elution positions of fluorescently labeled linear α -1,3-mannose polymers, from trimer (*far left*) to nonomer (*far right*).

cells in a volume of 50 μ l PBS were inoculated intranasally (39, 40). At 3 h and 7 days after inoculation animals were sacrificed, and the lungs, livers, spleens, and brains were removed, homogenized in PBS, and plated as serial dilutions on appropriate media for assessment of colony forming units (CFUs). Initial inocula were also plated to confirm CFUs.

RESULTS

To purify the cryptococcal α -1,3 mannosyltransferase we needed a rapid assay. A thin layer chromatography (TLC) based assay that was used initially (22) is time consuming and difficult to scale up. To address these problems we modified the dimannoside assay substrate with anthranilic acid (33, 41) to generate a fluorescent compound, and used HPLC to analyze reaction products. We similarly derivatized a ladder of mannose polymers generated from cryptococcal GXM to use as standards (Fig. 1, *diamonds*). When the modified substrate was incubated at 30 °C in the presence of cryptococcal membranes and nonradioactive GDP-mannose, a peak of fluorescent material was detected that comigrated with the trimer standard of the mannose ladder (Fig. 1, *black trace*). This peak was not present if either GDP-mannose (Fig. 1, *gray trace*) or cryptococcal membranes were omitted, or if incubation was performed on ice (not shown).

To confirm that the activities detected in crude membranes by the HPLC assay corresponded to those previously characterized by TLC (22) we examined the cation dependence of product formation. In the presence of Mn²⁺, cryptococcal membranes modify mannose- α -1,3-mannose to two products, with the majority containing mannose added in α -1,2 linkage, and the remainder modified with mannose in α -1,3 linkage. In contrast, in the presence of Co²⁺ the latter product, which corresponds to a subunit of the GXM structure, predominates (22). The relative amounts of α -1,2 and α -1,3 products formed in the presence of each cation were similar using either the HPLC or the TLC assay. Product identities were further confirmed by comigration with standards and mannosidase digestion (not shown).

We were curious about the prevalence of this activity, so we next examined product formation in several other fungal organisms. Membrane preparations of the ascomycetous fungi *S. cerevisiae* and *C. albicans* showed robust transfer of mannose in α -1,2-linkage to the substrate in standard assays, but only trace amounts of the α -1,3-linked product. However, membrane preparations of *Tremella mesenterica*, a non-pathogenic basidiomycetous fungus with a capsule similar to that of *C. neoformans* (43), generated a fully α -1,3-linked product. Properties of the mannosyltransferase activity in this organism were similar to that observed in cryptococcal membranes (data not shown).

We used fluorescent substrate and HPLC detection to purify the α -1,3-mannosyltransferase activity from a detergent ex-

TABLE I
A representative α -1,3-mannosyltransferase purification

Fraction	Specific activity	Fold purification	Yield
	<i>pmol/min/mg</i>		
P-100	3	1	100
TX-100 extract	3	1	57
Q-Sepharose	5	2	9
Source Q	100	20	10
Hydroxyapatite	800	270	5
Con A/Source Q	14,300	4800	2

tract of *C. neoformans* membranes. Although affinity resins such as GDP-hexanolamine Sepharose resolved this activity from the α -1,2-mannosyltransferase, yield was such that these were not ultimately useful for purification. Instead, conventional chromatography steps were employed to enrich the desired activity 5–10,000 fold over its presence in washed cryptococcal membranes (Table I). The final material had a pH optimum of 8 and was most active at 30 °C, with a linear increase in product formation until >90 min. Similar to the crude material, purified enzyme was active in the presence of Mn^{2+} , Co^{2+} , and Mg^{2+} in order of decreasing activity, with the Mg^{2+} value 80% of the value with Mn^{2+} . There was no activity in the presence of 0.1 mM EDTA without cation addition.

Prominent polypeptides in the most highly enriched fraction, obtained from Source 15Q chromatography of ConA eluted material (Fig. 2), were subjected to protein sequence analysis, both by direct N-terminal Edman sequencing and by tandem mass spectrometry analysis of internal peptides. The resulting peptide sequences were compared with predicted protein sequences of the entire cryptococcal genome, obtained by analysis of the TIGR *C. neoformans* genome data base (www.tigr.org/tdb/e2k1/cna1/index.shtml) using Twinscan software (www.cse.wustl.edu/~brent/Bio/MB-Lab-Software.htm (44)). Although gene prediction in *C. neoformans* is confounded by the multiple small introns typically present, internal exons are predicted with 78% sensitivity by this system. Mass spectrometry information on the size of tryptic fragments derived from each protein band was used to further support identifications (not shown).

The peptide sequence from the major band visible in the final Source 15Q fractions (Fig. 2) corresponded to a predicted protein with close homology to ubiquitin ligase, both by direct sequence (Table II, Band B) and by additional mass matches (not shown). This protein was considered unlikely to be the transferase under study and was not pursued further. Peptide sequences of two additional bands, present in roughly equal amounts in the most enriched fraction (Fig. 2, *single asterisk*), were of greater interest. These sequences (Table II, Bands A and C) corresponded to predicted proteins with strong homology to products of cryptococcal CAP genes. CAP genes were initially identified as defective in cryptococci lacking capsules after mutagenesis. Gene disruption studies of four of these have confirmed that they are required for capsule synthesis and for cryptococcal virulence, but the nature of the proteins they encode has not been elucidated (13–16).

We were excited by the homology of the two candidate proteins to CAP gene products, but needed to determine which one was responsible for the observed mannosyl transfer activity. As an initial screen we used double-stranded RNA interference (RNAi), which our lab has recently developed as a tool for specific gene silencing in *Cryptococcus* (34). This procedure is quite rapid, and does not require knowledge of the entire sequence of the gene or of the gene structure.

To test the candidate proteins, we cloned duplicate ~300-bp segments of either the CAP64 homolog or the CAP59 homolog such that upon transcription the RNA would form a hairpin

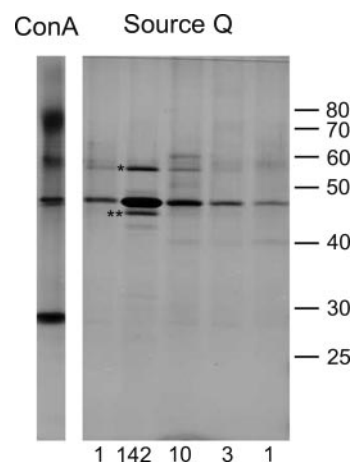


FIG. 2. Enriched mannosyltransferase fractions. A silver-stained SDS-PAGE gel of the ConA pool and second Source 15Q step fractions (see Table I) is shown. Values under the Source Q fraction lanes indicate relative activity in those samples. * and ** indicate polypeptides discussed in the text. Protein MW standards are in kDa.

TABLE II
Peptide sequence matches derived from the enriched mannosyltransferase preparation

Band	Method	Peptide sequence	Protein
A	MS-MS	KHYLISDTPGSR	Cap64p
A	MS-MS	KLTTTVGNIEIHYLR	Cap64p
B	MS-MS	RNNPSLLSGSFLLIR	ubiquitin ligase
C	MS-MS	RNTALAPLWQGEQDK	Cap59p
C	EDMAN	VIHTKDLFLERLALNATSEAF	Cap59p
C	MS-MS	LEPFQV	Cap59p

structure, with the stem composed of double-stranded RNA corresponding to that segment (see “Experimental Procedures” and Refs. 34 and 45 for details and diagrams). This double-stranded RNA serves to initiate specific destruction of the corresponding mRNA (recently reviewed in Ref. 46). We expressed each construct (or the vector alone) in a *C. neoformans* strain that is wild type for capsule formation. Targeting of each gene resulted in >90% reduction in the corresponding mRNA, while vector alone or the other construct caused no change (RNA blot not shown).

We next compared membrane preparations of cells carrying the various RNA interference constructs for transferase activity. Cells expressing the empty vector demonstrated wild type activity, as expected (Fig. 3A, *gray trace*). The same pattern (Fig. 3A, *black trace*) was seen in cells in which RNA interference targeted the CAP64 homolog (Fig. 2, *asterisk* and Table II, Band A). In contrast, cells expressing the construct designed to interfere with the CAP59 homolog (Fig. 2, *double asterisk* and Table II, Band C) showed no activity in our standard assay (Fig. 3B, *black trace*). Selection against maintenance of the URA5 marked interference plasmid, by growth in the presence of 5-FOA, restored the activity to normal (Fig. 3B, *gray trace*). These results suggested that the CAP59 homolog, rather than the CAP64 homolog, encodes the α -1,3-mannosyltransferase.

We next assessed the capsule phenotype of cells in which the α -1,3-mannosyltransferase activity was reduced by interference. Indirect immunofluorescence experiments using anticapsular monoclonal antibodies suggested reduced labeling of capsule (not shown). For higher resolution analysis we examined the capsule by thin-section electron microscopy after immunolabeling with gold-conjugated monoclonal antibodies to capsule (Fig. 4). Wild type cells transformed with a control plasmid targeting an auxotrophic marker demonstrate fibrillar capsule structures heavily labeled with gold particles (*panel A*). In

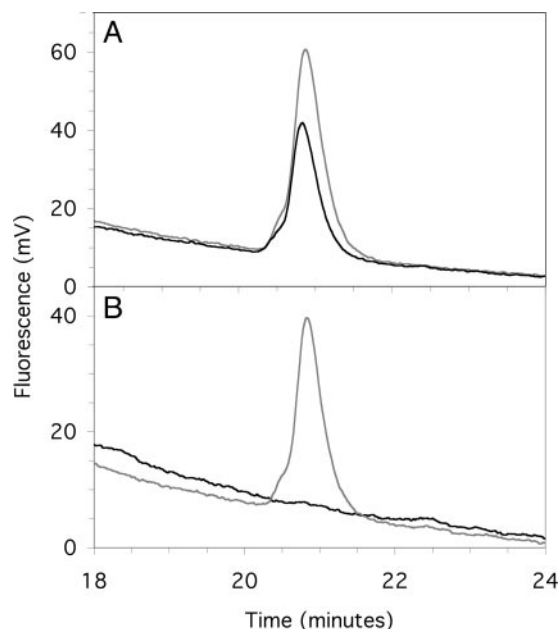


FIG. 3. Double-stranded RNA interference analysis of candidate mannosyltransferases. Membrane preparations from *C. neoformans* cells were analyzed by the standard assay using Program 2. *Panel A*, cells with the RNAi vector alone (*gray trace*) or cells with RNAi targeting the *CAP64* homolog (*black trace*). *Panel B*, cells with RNAi targeting the *CAP59* homolog (*black trace*) or the same strain after growth on 5-FOA to select against plasmid maintenance (*gray trace*).

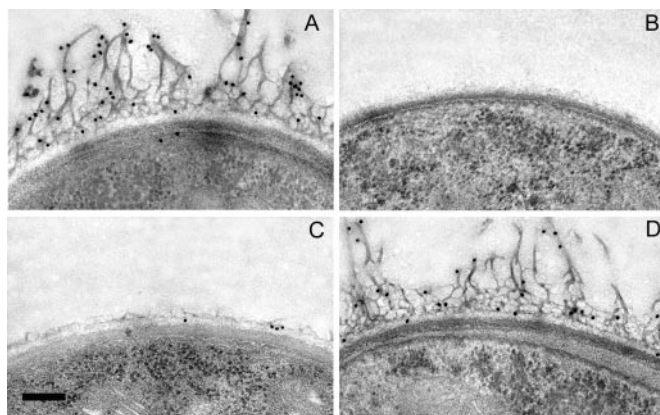


FIG. 4. Immunogold labeling of *C. neoformans* capsule. Cells transformed with the plasmids indicated were fixed, sectioned, and exposed to monoclonal antibody 2H1 as under “Experimental Procedures.” *Panel A*, pADE2i; *panel B*, pCAP59/ADE2i; *panel C*, pCMT1/ADE2i; *panel D*, cells as in *C*, grown in 5-FOA. Scale bar, 0.2 μ m.

contrast, cells expressing an interference plasmid targeting *CAP59* demonstrate neither capsule structures nor labeling with anti-capsular antibody (*panel B*), as expected because this gene is required for capsule synthesis (13). Cells in which RNA interference targeted expression of the putative mannosyltransferase were also deficient in capsule structures and antibody labeling (*panel C*). Over 50% of these cells had no visible capsule, although occasionally small amounts were detected by antibody labeling. The remainder had detectable capsule, but this had lower density and shorter fibers than wild type. In contrast, over 95% of wild type cells had completely normal capsule. Upon loss of the interference plasmid all of the cells regained a completely normal appearance, with uniformly well-labeled fibrillar capsules (*panel D*), and wild type enzyme activity (Fig. 3*B*, *gray trace*).

To obtain the cDNA sequence encoding the α -1,3-mannosyltransferase, now termed Cmt1p for cryptococcal mannosyltrans-

MFRNTRLRTPFRPATPSLPTSSHSPIARASLSKSPFLFVLSLVLVLCIF
FLSFLSHDPDSARKLQWPGLFSPSPSVIHTKDLFLERALNATSEA
 FREICPSAGDPVHLD**DPDL**TEAQKKRYLPLKRSKRGRYLLVTNTRQI
 EAHLDDLNTLIVLLRYLAPDHLAVSILEGPDSDCTQKAIEQVLKP
 MLDDQGLSAWTRIEETGESKIDWCKHNRIEKIAELRNALAPLWQG
 EGDQKWGDEIEAVVFFNDVYLHAADILELVYQHVKNAGITTTAMDW
 WKKRPEYYYDVVWVGRITDGTDLFYPIDNPWWSPSSDLFPNSPNSRN
 AYSRLE**FPQV**FSSWNALAVLSPKPFLPPHNVRFRRGDVEKGECAAS
 ECTLIATDFWKAGFGKVAVVPSVQLAYERDVAKDIIEEDVGKQKEQL
 GWIDGVPEHLDDKIEWSTKPKPKVRCHPWPEVNGLSANVWEETRW
 VQPWLE

FIG. 5. Predicted sequence of Cmt1p. The putative membrane-spanning region is in *bold type*, and regions corresponding to sequenced peptides (see Table II) are *underlined*. A potential site of *N*-glycosylation is *double-underlined*, as is the sequence DPD. N-terminal protein sequencing of material purified from *C. neoformans* yielded the peptide sequence beginning with VIHT.

ferase, we used available cryptococcal sequence to design primers, and performed RACE (see “Experimental Procedures”). The predicted 53-kDa translation product of *CMT1* (Fig. 5) is homologous to the predicted product of *C. neoformans* *CAP59* (GenBank™ A56055), with 35% of residues identical and 54% positive over the most homologous 276 amino acids (beginning with residue 123 of Cmt1p, corresponding to residue 89 of Cap59p). The sequence is consistent with the typical type II transmembrane structure of membrane associated sugar transferases, with a potential *N*-glycosylation site on the predicted luminal domain. Interestingly, the N-terminal protein sequencing indicated that the protein that was purified from *C. neoformans* was truncated, missing the N-terminal soluble domain, membrane-spanning sequence, and 22 additional amino acids (Fig. 5).

To confirm that *CMT1* encoded the activity of interest we expressed the truncated form of the protein (beginning at the underlined peptide *VIHT* in Fig. 5), modified with a N-terminal His₆ tag, in *S. cerevisiae*. Immunoblotting with anti-His antibody confirmed expression of the protein (Fig. 6, *inset*). *S. cerevisiae* containing only the expression vector showed a large peak representing α -1,2-mannosyl transfer, but only small amounts of the α -1,3 product (Fig. 6, *gray trace*). The latter is presumably made by a different enzyme that can modify this substrate, as *S. cerevisiae* has no homolog of Cmt1p. The same cells expressing *CMT1* exhibited a dramatic increase in the α -1,3 product, while the α -1,2 product was not changed (Fig. 6, *black trace*). Although this N-terminal truncation was active, the activity was lost when 14 amino acids were deleted from the C terminus (not shown).

Cells in which we had down-regulated *CMT1* expression by RNA interference showed no mannosyltransferase activity and greatly reduced capsule associated with cells. We wished to confirm these observations in a strain where the gene had been disrupted, and to test whether there would be any alteration in virulence of such cells. To do this we generated a strain of *C. neoformans* in which the *CMT1* gene was disrupted with an auxotrophic marker (Fig. 7), and additional strains in which this disruption was complemented with an exogenous copy of *CMT1*. The disrupted strain displayed no α -1,3-mannosyltransferase activity (Fig. 8), although activity was restored in the complemented strains (not shown). We next compared the ability of parental, disrupted, and complemented disruption strains, which all grew at equivalent rates *in vitro*, to infect C57Bl/6 mice. Using an inhalational model of cryptococcosis we found no defect in virulence of the disrupted strain (not shown). There was also no alteration in the capsule of this strain, as assessed by electron microscopy (see “Discussion”). To rule out the possibility that this result was due to a truncated protein with residual activity, we constructed an additional strain in

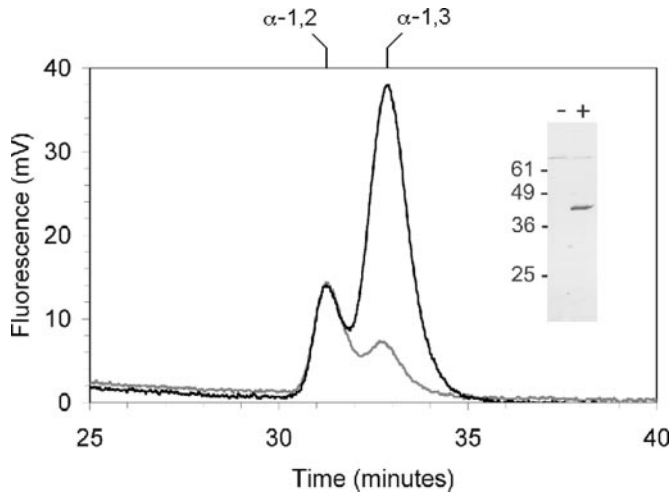


FIG. 6. **Expression of Cmt1p in *S. cerevisiae*.** Membrane preparations from *S. cerevisiae* cells containing vector alone (gray trace) or expressing Cmt1p as described under "Experimental Procedures" (black trace) were analyzed in the standard assay, and the products analyzed using Program 3. Elution positions of the two trimer products generated in crude membranes from the α -1,3-dimannose assay substrate are indicated above. Inset, an anti-His antibody immunoblot of equal amounts of total protein from *S. cerevisiae* without (-) or with (+) Cmt1p expression.

which the entire *CMT1* coding region was deleted. Like the disruption, these cells lacked α -1,3-mannosyltransferase activity but bore normal capsule (electron microscopy not shown).

DISCUSSION

We have purified an α -1,3-mannosyltransferase from *C. neoformans*, and have cloned the corresponding gene, *CMT1*. Expression of the protein in a heterologous system demonstrates that this gene indeed encodes the structural gene for this enzyme, and the activity is appropriate for a role in capsule synthesis. The only homology Cmt1p has to known proteins predicted by the non-redundant NCBI data base, notably including the model yeast *S. cerevisiae*, is to the predicted product of *C. neoformans* CAP59 (GenBank™ accession number L26508). Cap59p is a protein of unknown function, which is required for capsule synthesis. The demonstration that Cmt1p is a mannosyltransferase suggests that perhaps Cap59p also acts in glycan synthesis. Searches of the limited genomic data available for other fungi suggest that additional homologs of CAP59 exist in several species, including the non-pathogenic *Neurospora crassa*, the plant pathogen *Magnaportha grisea*, and the mammalian pathogen *Histoplasma capsulatum*. These species do not produce capsule, so it will be interesting to examine whether these genes are expressed, and the functions of the enzymes they encode.

Cmt1p has the type II membrane protein structure expected of a transferase that functions in formation of an extracellular glycoconjugate. Consistent with observations on other transferases, the cytosolic and transmembrane domains are not required for activity of Cmt1p, but may function in protein localization. The protein as purified was truncated at the N terminus, but it remains to be determined at what point in protein maturation or purification this occurs. Deletion of 14 amino acids from the C terminus abolished activity. Cmt1p also has sequence motifs associated with enzymes that bind nucleotide derivatives (Rossmann fold) or are involved in glycosyl transfer (DXD motif, Ref. 47), although the latter is not present in a canonical context.

In all steps of Cmt1p purification, it co-purified with a second polypeptide of similar abundance, which also bears strong homology to a member of the CAP gene family. RNA interference

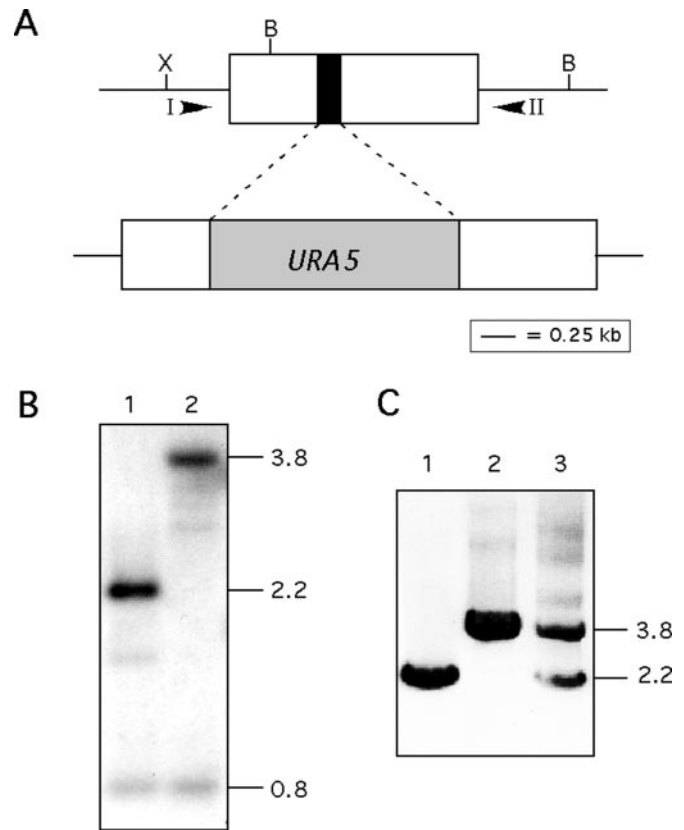


FIG. 7. **Generation of a *CMT1* disruption.** Panel A, diagram of the disruption strategy, in which 0.2 kb (black box) of the *CMT1* coding sequence (white) was replaced with the 1.8-kb *URA5* gene (gray). Panel B, DNA blot. Total genomic DNA from parental (1) or disruption (2) strains was cut with BamHI (B) and XhoI (X) and probed with the *CMT1* coding sequence. Fragment sizes are indicated in kb. Panel C, PCR of the parental (1), disruption (2), or corrected (3) strains with primers I and II (see panel A). Additional PCR reactions using a forward primer 0.4-kb upstream of *CMT1* and a reverse primer within *URA5* yielded a product in the disruption and corrected strains, but not in the parent (not shown).

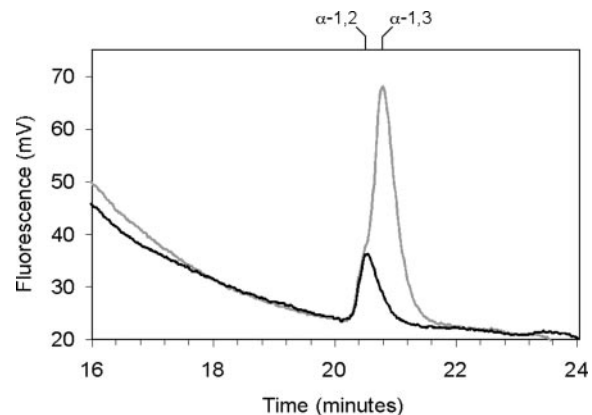


FIG. 8. **Cells disrupted in *CMT1* lack α -1,3-mannosyltransferase activity.** Membrane preparations of the *C. neoformans* parental strain (gray trace) or the same strain disrupted in *CMT1* (black trace) were tested in the standard assay, and the products analyzed using Program 2. Although this program does not fully resolve the α -1,2-linked trimer (shoulder in gray trace) from the product in α -1,3-linkage, it is clear that the latter is no longer made in the disrupted strain.

targeting the gene encoding the second protein did not alter mannosyltransferase activity or overall capsule morphology. However, the co-purification of two CAP protein homologs suggests that these polypeptides might normally be associated. There is certainly precedent for multienzyme complexes acting

in fungal glycan synthesis (48–50). Fully dissecting the individual roles of these proteins, and any additional binding partners, will require isolation of the putative complex from *C. neoformans* and examination of each component.

Gene disruption, gene deletion, and RNA interference targeting *CMT1* all yielded cells devoid of activity by our standard assay, consistent with the Cmt1p function as demonstrated by heterologous expression. However, we were surprised to find a difference in capsule phenotype between cells in which *CMT1* was targeted by RNA interference and those in which the gene was disrupted or deleted. As RNA interference acts post-transcriptionally, and lowers the pool of specific mRNA without totally eliminating it, we had expected that disruption or deletion of *CMT1* might enhance the altered capsule phenotype. In contrast, these mutants bore apparently normal capsule, despite lacking Cmt1p enzyme activity.

RNA interference clearly targeted the mannosyltransferase of interest, as shown by the lack of Cmt1p activity. However, it is likely that it also reduced production of another message, resulting in the observed capsule phenotype. Several recent studies have addressed the issue of such off-target interference (51, 52). It appears that, although the interference process itself is mediated by small interfering RNAs (siRNA) of about 20 nucleotides in length, off-target interference may be mediated by shorter regions of homology. In one report, as few as 11 contiguous nucleotides appear sufficient to direct silencing of unintended targets (51). Comparison of our interference segment to the cryptococcal data base yields 17 sequences that are predicted to encode proteins and contain 12 or more contiguous nucleotides of identity. It is possible that silencing of one or more of these genes is responsible for the observed capsule phenotype; this will be addressed in future studies.

Deletion of *CMT1* yields cells that have no activity in our standard assay, yet still make capsule. What, then, is the role of this protein? One consideration is the propensity of fungi to have multiple enzymes of overlapping specificity involved in glycan synthesis (42, 53). Given the complexity and importance of the capsule, it is likely that there are redundant proteins that can generate the GXM backbone, perhaps normally acting under different growth conditions or upon different substrates, but able to compensate for the loss of Cmt1p. Differences in substrate specificity might be such that only Cmt1p can act on an anthranilic acid-derivatized mannose dimer substrate under the conditions of our standard assay. This could result in normal capsule synthesis despite a reduction in measurable activity. Alternatively, it may be that the main function of Cmt1p is not directly related to GXM synthesis. Additional studies of this protein, its homologs, and its binding partners should help to answer these questions.

Acknowledgments—We thank Bob Haltiwanger and Jochen Buck for advice and encouragement in early stages of this project; Randy Brown, Aaron Tenney, and Michael Brent for help with Twinscan; Wandy Beatty and Lori LaRose for electron microscopy; and David Haydon at Oxford Glycosciences for mass spectrometry analysis of peptides. We thank Ken Blumer, Arturo Casadevall, Robert Cherniak, Jerry Hart, Joe Heitman, Tom Kozel, and Randy Schekman for strains and reagents, and the Biochemistry Department at Washington University Medical School for fermenter use. We greatly appreciate useful discussions with Eva Istvan, Uwe Himmelreich, and members of the Doering laboratory, and we thank Bob Haltiwanger, Jeramia Ory, and Stacey Klutts for comments on the article.

REFERENCES

- Casadevall, A., and Perfect, J. R. (1998) *Cryptococcus neoformans*, American Society for Microbiology, Washington, D. C.
- Bose, I., Reese, A. J., Ory, J. J., Janbon, G., and Doering, T. L. (2003) *Eukaryot. Cell* **2**, 655–663
- Buchanan, K. L., and Murphy, J. W. (1998) *Emerg. Infect. Dis.* **4**, 71–83
- Feldmesser, M., Rivera, J., Kress, Y., Kozel, T. R., and Casadevall, A. (2000) *Infect. Immun.* **68**, 3642–3650
- Cherniak, R., Valafar, H., Morris, L. C., and Valafar, F. (1998) *Clin. Diagn. Lab. Immunol.* **5**, 146–159
- Vaishnav, V. V., Bacon, B. E., O'Neill, M. O., and Cherniak, R. (1998) *Carb. Res.* **306**, 315–330
- Fromtling, R. A., Shadomy, H. J., and Jacobson, E. S. (1982) *Mycopathologia* **79**, 23–29
- Jacobson, E. S., Ayers, D. J., Harrell, A. C., and Nicholas, C. C. (1982) *J. Bacteriol.* **150**, 1292–1296
- Janbon, G., Himmelreich, U., Moyrand, F., Improvisi, L., and Dromer, F. (2001) *Mol. Microbiol.* **42**, 453–467
- Moyrand, F., Klaproth, B., Himmelreich, U., Dromer, F., and Janbon, G. (2002) *Mol. Microbiol.* **45**, 837–849
- Kozel, T. R., Levitz, S. M., Dromer, F., Gates, M. A., Thorkildson, P., and Janbon, G. (2003) *Infect. Immun.* **71**, 2868–2875
- Cleare, W., Cherniak, R., and Casadevall, A. (1999) *Infect. Immun.* **67**, 3096–3107
- Chang, Y. C., and Kwon-Chung, K. J. (1994) *Mol. Cell. Biol.* **14**, 4912–4919
- Chang, Y. C., Penoyer, L. A., and Kwon-Chung, K. J. (1996) *Infect. Immun.* **64**, 1977–1983
- Chang, Y. C., and Kwon-Chung, K. J. (1998) *Infect. Immun.* **66**, 2230–2236
- Chang, Y. C., and Kwon-Chung, K. J. (1999) *J. Bacteriol.* **181**, 5636–5643
- White, C. W., and Jacobson, E. S. (1993) *Can. J. Microbiol.* **39**, 129–133
- White, C. W., Cherniak, R., and Jacobson, E. S. (1990) *J. Med. Vet. Mycol.* **28**, 289–301
- Jacobson, E. S., and Payne, W. R. (1982) *J. Bacteriol.* **152**, 932–934
- Wills, E. A., Roberts, I. S., del Poeta, M., Rivera, J., Casadevall, A., Cox, G. M., and Perfect, J. R. (2001) *Mol. Microbiol.* **40**, 610–620
- Bar-Peled, M., Griffith, C. L., and Doering, T. L. (2001) *Proc. Natl. Acad. Sci. U. S. A.* **98**, 12003–12008
- Doering, T. L. (1999) *J. Bacteriol.* **181**, 5482–5488
- Heitman, J., Casadevall, A., Lodge, J. K., and Perfect, J. R. (1999) *Mycopathologia* **148**, 1–7
- Varki, A., Cummings, R., Esko, J., Freeze, H., Hart, G., and Marth, J. (eds) (1999) *Essentials of Glycobiology*, p. 258, Cold Spring Harbor Laboratory Press, Cold Spring Harbor, NY
- Dean, N. (1999) *Biochim. Biophys. Acta* **1426**, 309–322
- Strahl-Bolsinger, S., Gentzsch, M., and Tanner, W. (1999) *Biochim. Biophys. Acta* **1426**, 297–307
- Orlean, P. (1992) *Biochem. Cell Biol.* **70**, 438–447
- Robbins, P. W. (1991) *Biochem. Soc. Trans.* **19**, 642–645
- Sentandreu, R., Herrero, E., Martinez-Garcia, J. P., and Larriba, G. (1984) *Subcell Biochem.* **10**, 193–235
- Mukherjee, S., Lee, S., Mukherjee, J., Scharff, M. D., and Casadevall, A. (1994) *Infect. Immun.* **62**, 1079–1088
- Duro, R. M., Netski, D., Thorkildson, P., and Kozel, T. R. (2003) *Clin. Diagn. Lab. Immunol.* **10**, 252–258
- Ausubel, F. M., Brent, R., Kingston, R. E., Moore, D. D., Seidman, J. G., Smith, J. A., Struhl, K., Albritton, L. M., Coen, D. M., and Varki, A. (2003) in *Current Protocols in Molecular Biology* (Chanda, V. B., ed) Vol. 2, p. 13.1.4, John Wiley & Sons, Inc., New York
- Anamula, K. R., and Dhume, S. T. (1998) *Glycobiology* **8**, 685–694
- Liu, H., Cottrell, T. R., Pierini, L. M., Goldman, W. E., and Doering, T. L. (2002) *Genetics* **160**, 463–470
- Kang, Y. S., Kane, J., Kurjan, J., Stadel, J. M., and Tipper, D. J. (1990) *Mol. Cell. Biol.* **10**, 2582–2590
- Davidson, R. C., Blankenship, J. R., Kraus, P. R., De Jesus Berrios, M., Hull, C. M., D'Souza, C. A., Wang, P., and Heitman, J. (2002) *Microbiology* **148**, 2607–2615
- Davidson, R. C., Cruz, M. C., Sia, R. A. L., Allen, B., Alspaugh, J. A., and Heitman, J. (2000) *Fungal Genet. Biol.* **29**, 38–40
- Toffaletti, D. L., Rude, T. H., Johnston, S. A., Durack, D. T., and Perfect, J. R. (1993) *J. Bacteriol.* **175**, 1405–1411
- Cox, G. M., Mukherjee, J., Cole, G. T., Casadevall, A., and Perfect, J. R. (2000) *Infect. Immun.* **68**, 443–448
- Wilder, J. A., Olson, G. K., Chang, Y. C., Kwon-Chung, K. J., and Lipscomb, M. F. (2002) *Am. J. Respir. Cell Mol. Biol.* **26**, 306–314
- Anumula, K. R. (1994) *Anal. Biochem.* **220**, 275–283
- Roncero, C. (2002) *Curr. Genet.* **41**, 367–378
- Fraser, C. G., Jennings, H. J., and Moyna, P. (1973) *Can. J. Biochem.* **51**, 219–224
- Korf, I., Flicek, P., Duan, D., and Brent, M. R. (2001) *Bioinformatics* **17**, Suppl. 1, S140–S148
- Cottrell, T. R., and Doering, T. L. (2003) *Trends Microbiol.* **11**, 37–43
- Denli, A. M., and Hannon, G. J. (2003) *Trends Biochem. Sci.* **28**, 196–201
- Wiggins, C. A., and Munro, S. (1998) *Proc. Natl. Acad. Sci. U. S. A.* **95**, 7945–7950
- Jungmann, J., and Munro, S. (1998) *EMBO J.* **17**, 423–434
- Jungmann, J., Rayner, J. C., and Munro, S. (1999) *J. Biol. Chem.* **274**, 6579–6585
- Girrbach, V., and Strahl, S. (2003) *J. Biol. Chem.* **278**, 12554–12562
- Jackson, A. L., Bartz, S. R., Schelter, J., Kobayashi, S. V., Burchard, J., Mao, M., Li, B., Cavet, G., and Linsley, P. S. (2003) *Nat. Biotechnol.* **21**, 635–637
- Chi, J. T., Chang, H. Y., Wang, N. N., Chang, D. S., Dunphy, N., and Brown, P. O. (2003) *Proc. Natl. Acad. Sci. U. S. A.* **100**, 6343–6346
- Hochstenbach, F., Klis, F. M., van den Ende, H., van Donselaar, E., Peters, P. J., and Klausner, R. D. (1998) *Proc. Natl. Acad. Sci. U. S. A.* **95**, 9161–9166

